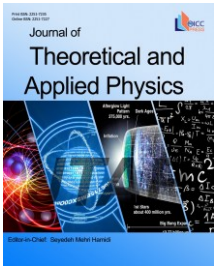

J. Theor. Appl. Phys., 2026; 20(2): 132-140

Journal of Theoretical and Applied Physics (JTAP)

https://doi.org/10.57647/jtap.2026.2002.10

Research Article

Rashba Coupling Assisted Negative Differential Conductance in Graphene Based Quantum Antidot Nano-Ribbon

Kobra Hasanirokh[1], Neda Shahabi[1,2*], Arash Phirouznia[1,2]

[1]*Department of Physics, Azarbaijan Shahid Madani University, 53714-161, Tabriz, Iran*
[2]*Condensed Matter Computational Research Lab. Azarbaijan Shahid Madani University, 53714-161, Tabriz, Iran*

***Corresponding author:** Nedashahabi63@gmail.com

Article History:

Received:
16 January 2025

Revised:
27 July 2025

Accepted:
17 December 2025

Published Online:
05 February 2026

Published in Issue:
30 April 2026

Abstract

Characteristic quantum transport features of a graphene-based quantum antidot structure which has been considered between two semi-infinite zig-zag graphene leads is investigated theoretically. The RPA-Keldysh method has been employed to capture Colomb interaction between the carriers in the presence of the Rashba interaction. It has been realized that the Colomb interaction results in negative differential conductance (NDC) which significantly depends on the strength of the Rashba coupling.

Keywords: RPA-Keldysh approach; Rashba interaction; Quantum transport; Spintronics

Cite this article: Hasanirokh, K., Shahabi, N., Phirouznia, A., (2026). Rashba Coupling Assisted Negative Differential Conductance in Graphene Based Quantum Antidot Nano-Ribbon. *J. Theor. Appl. Phys.,* 20(2), 132-140. https://doi.org/10.57647/jtap.2026.2002.10

1. Introduction

The possibility of forming graphene antidot lattice has been investigated in several studies more than a decade ago [1–3] where e-beam lithography has been proposed to carve graphene nanoribbons [1]. It has been shown that this antidot structure turns the semi-metallic graphene into a gapped semiconductor, in which the size of the gap can be manipulate by the antidot lattice parameters [1, 2]. Meanwhile for an antidot lattice on zigzag graphene-based nanoribbon Fano resonances have been reported when the antidots are located on the ribbon edges [2].

Spin-orbit (SO) interactions in graphene-based nanostructures could lead to interesting effects regarding the fact that extrinsic SO interaction in graphene is relatively high [4]. Meanwhile, these type of interactions in the graphene-based and also graphene-like structures results in very interesting spintronics related effects [5–8]. Spin-orbit interactions are a promising key ingredient in the spintronics and the importance of these type of

interactions in low dimensional system such as a mono-layer graphene is an universal subject matter. Intrinsic spin-orbit (ISO) interaction originates from the carbon intra-atomic SO interaction and not only can open a gap but due to localized edge states it gives a quantum spin Hall phase [9]. The extrinsic Rashba SO interaction [10] arises by breaking the structure inversion symmetry, possibly caused by substrate [11–14] or curvature results [15], adsorbed adatoms [16–19], vertical
external electric fields [20, 21], etc. It has been shown that an impurity induces the sp^3 distortion in graphene structure which the latter leads to a large increase in the magnitude of the spin-orbit coupling [18]. It was found that the Rashba SO interaction tends to close gap and leads to a splitting of the Dirac points into four identical points [22, 23] in which this splitting is missed in the low energy calculations [9]. It was also shown that the Rashba spin-orbit coupling removes the electron-hole band symmetry [24]. Furthermore, it was also shown that in a graphene sheet, the interplay between the intrinsic and the Rashba spin-orbit couplings breaks the symmetry of the electron-hole energy dispersion as long as the magnitude of one SOC mechanism becomes zero [24].

It is interesting to know that the Rashba coupling in graphene can be tuned to much high values. For example the Rashba coupling constant can raise to 0.2 eV [12] which could be considered a relatively high SO interaction as compared to the Rashba coupling strength in other structures. Meanwhile it should be noted that the Rashba interaction could be controlled by an applied gate voltage.

In the present study, it was shown that the Coulomb interaction results in negative differential conductance in the presence of the Rashba coupling. Here, we have also identified a mechanism for modulating negative conductance by the Rashba interaction in the graphene based quantum antidot systems.

Here we have focused on treating the Colomb interaction within the RPA-Keldysh approach which as we have demonstrated, a Rashba coupling dependent NDC in the graphene nanoribbons containing a single anti-dot. Meanwhile, there are various articles in this field which discovered other aspects of graphene and silicene nanostructures, focusing on their electronic, transport, and thermoelectric properties. Pedersen et al investigated graphene antidot lattices, highlighting their potential for designing defects and spin qubits [1]. Zhang et al. analyzed the band structures and transport properties of zigzag graphene nanoribbons with antidot arrays, emphasizing their tunable electronic behavior [25]. Manchon et al. provided new insights into Rashba spin-orbit coupling, discussing its implications for spintronics [26]. Kalami et al examined the role of linear defects and quantum antidot arrays in armchair-edge silicene nanoribbons, demonstrating their significant impact on electronic and thermoelectric properties [27]. These studies collectively prepared a clear and understanding of low-dimensional materials for potential applications in nanoelectronics and quantum technologies.

In addition, Kalami et al have studied the influence of different shapes and sizes of antidots on the transport and electrical properties of armchair graphene nano-ribbons. According to their results, the fewer the number of extracted atoms and the more symmetrical the shape of the quantum antidot, the smaller the energy band gap will be [28]. Here we need to point out that the fabrication of graphene antidote lattices has been reported in several experimental investigations. In 2006, Berger et al have reported the construction of patterned epitaxial graphene using standard nanolithography methods [29]. Likewise, Pedersen et al in [1] and Shen et al in [30] utilized electron beam lithography to carve graphene structure in order to create antidots on its surface. In a similar way, Kato et al fabricated antidote lattice samples from GaAs/AlGaAs wafers by shallow wet chemical etching by means of e-beam lithography [31].

2. Model and approach

We have employed the non-equilibrium Keldysh formalism and the random-phase approximation (RPA) for electronic quantum transport. This approach has been developed in [32, 33] in which the electron-electron interaction has been treated within the RPA coupled with the formal NEGF formalism. We have started with tight-binding Hamiltonian of a graphene-based quantum antidot system depicted in Figure 1.

The central region (C) has been assumed to be coupled adiabatically with a time-dependent smooth switching $\eta(t)$ to the noninteracting semi-infinite leads. An adiabatic coupling means that $\eta(t)$ vanishes in the far past and the steady-state current is calculated in the long-time limit. We have denoted the on-site energies of the central region by ϵ_n and the creation/annihilation operators in the central region is $a^{\dagger}{}_n/a_n$ (where n labels the site number in the central region). The system Hamiltonian is then given by:

$$\mathrm{H(t)} = \mathrm{H_c} + \mathrm{H_L} + \eta(\mathrm{t})(\mathrm{H_{CL}} + \mathrm{H_{int}}) \quad (1)$$

in which

$$H_c = H_0 + H_R \quad (2)$$

H_0 and H_R are the tight-binding Hamiltonian of the graphene and the Rashba spin-orbit interaction respectively.

$$H_0 = \sum_{l,m\in C} (\epsilon_l \delta_{lm} + t_{lm}) a_l^{\dagger} a_m \quad (3)$$

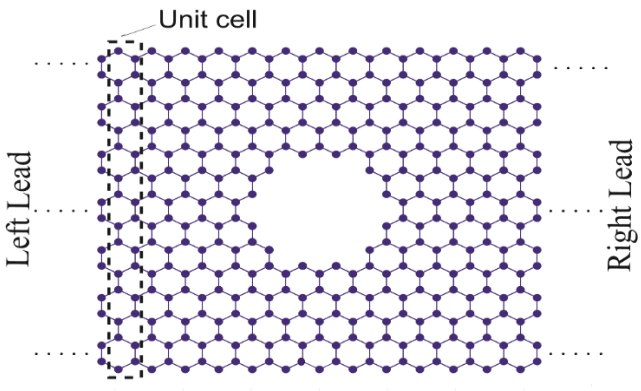

Figure 1. Schematic of the antidot graphene structure including N=316 carbon atoms in the central region. Dashed square represents the unit cell of the semi-infinite leads

In Eq. (3), t_{lm} is the nearest neighbor hopping amplitude and the on-site energy has been denoted by ϵ_l. $\eta(t)$ switches smoothly both of the coupling of the central region to the leads and the electron-electron interaction. This means that the influence of the initial correlations could be ignored in the final results [34, 35]. This approximation is permitted when the system gains a steady state in the longtime limit. Rashba spin-orbit interaction in graphene is defined as follows [22]:

$$H_R = it_R \sum_{<l,m>\in C} a_l^{\dagger}\left(\boldsymbol{s}\times\hat{\boldsymbol{d}}_{lm}\right).\hat{z}a_m + h.c \tag{4}$$

In which the vector **s** is the Pauli matrix representing the electron spin, the unit vector $\hat{d}_{lm}$ connects the sites l and m in the honeycomb lattice and <,> indicates the nearest neighbor summation in the central region. It should be noted that the Rashba strength has been assumed to be zero inside the leads.

The second and third term in Eq. (1) are given as follows,

$$H_L = \sum_{\alpha}\sum_{<i,j>\in L_\alpha} v_\alpha f_{\alpha i}^{\dagger} f_{\alpha j}$$

$$H_{CL} = \sum_{i\in L_\alpha}\sum_{l\in C}\left(V_{il}^{\alpha} f_{\alpha i}^{\dagger} a_j + H.c.\right) \tag{5}$$

$$H_{int} = \frac{U}{2}\sum_{l\neq m}\frac{\hat{n}_l\hat{n}_m}{|r_l - r_m|}$$

In which H_L is the leads Hamiltonian, $f_{\alpha i}^{\dagger}$ is the electron creation operator in the lead, i and j denote different sites in lead and v_α is the hopping energy in the leads. H_{CL} indicates the coupling of the central region and the leads V_{il}^{α} is the nearest neighbors hopping parameter between the corresponding sites of the lead $\alpha(i \in L_\alpha)$ and the central region ($l \in C$).

The Hamiltonian H_{int} defines the Coulomb interaction between charged carriers. $\hat{n}_l = a_l^{\dagger} a_l$ denotes the number operator of the lth site. It was assumed that density-density correlation function of the carriers is weak which so that $U < \hat{n}_l\hat{n}_m > \approx 0.1t$ in which l and m are the site indexes.

One can define the retarded Green's function of a semi-infinite lead as:

$$g_\alpha^R = \left[(E + i0)I - H_{L_\alpha}\right]^{-1} \tag{6}$$

In which the real space representation of g_α^R for the left and right isolated leads (indicated by the $\alpha = l,r$ respectively). Surface Green's function of the leads, $g_{\alpha s}$, has been approximated as described in [36]. Then the retarded and advanced self-energies for each lead are given as follows

$$\Sigma_\alpha^R = V_\alpha^{\dagger} g_{\alpha s}^R V_\alpha, \qquad \Sigma_\alpha^A = \Sigma_\alpha^{R\dagger} \tag{7}$$

in which $g_{s\alpha}^R$ is the retarded surface Green's function of the semi-infinite lead α (left / right).

Retarded Green's function and the lesser self-energy are given by

$$G^{R(\lambda\lambda')}(E) = \frac{1}{(E + i\eta)I - H_c - \Sigma_L^R - \Sigma_R^R}$$
$$\Sigma^{<(\lambda\lambda')}(E) = i\left(f_L\Gamma_L^{(\lambda\lambda')} + f_R\Gamma_R^{(\lambda\lambda')}\right) \tag{8}$$

Γ_α is the line width which is given by

$$\Gamma_\alpha^{(\lambda\lambda')}(E) = i\left(\Sigma_\alpha^{R(\lambda\lambda')}(E) - \Sigma_\alpha^{A(\lambda\lambda')}(E)\right) \tag{9}$$

in which E and $f_{L(R)}(E) = (\exp(E - (+)ev/2)/K_BT + 1)^{-1}$ are the energy of an injecting electron and α is the lead index and the Fermi distribution function in the lead α, respectively. λ and λ' (= ±1) being the z-component of the electron spin and v is the bias voltage.

The lesser and greater Green's functions are also defined as:

$$G^{<(\lambda\lambda')}(E) = G^{R(\lambda\lambda')}(E)\Sigma^{<(\lambda\lambda')}(E)G^{A(\lambda\lambda')}(E) \tag{10}$$

$$G^{A(\lambda\lambda')}(E) = G^{R(\lambda\lambda')}(E)^{\dagger} \tag{11}$$

$$G^{>(\lambda\lambda')}(E) = G^{<(\lambda\lambda')}(E) + 2iIm\left[G^{R(\lambda\lambda')}(E)\right] \tag{12}$$

The Coulomb interaction could be treated perturbatively within the spin-dependent Dyson formalism,

$$G^{R(\lambda\lambda')} = G_0^R + G_0^R(\Sigma_L^R + \Sigma_I^R)G^R \tag{13}$$

$$G^{<(\lambda\lambda')} = G^R(\Sigma_L^< + \Sigma_I^<)G^A \tag{14}$$

where $G_0^{R,<}$ is the Green function's of the isolated noninteracting system and Σ_I is the self-energy of the Coulomb interaction.

Effective Green's function is given by the Dyson equation in Keldysh space.
Lesser, greater and retarded components of Π are defined as

$$\Pi_{kl}^{<,>(\lambda\lambda')}(E) = \frac{-1}{2i}\int dE' G_{eff,kl}^{<,>(\lambda\lambda')}(E') G_{eff,lk}^{>,<(\lambda\lambda')}(E'-E) \quad (15)$$

and

$$\Pi^{R(\lambda\lambda')}(E) = \frac{1}{2\pi}\int dE' \frac{\Pi^{>(\lambda\lambda')}(E') - \Pi^{<(\lambda\lambda')}(E')}{E-E'+i0} \quad (16)$$

k and l indicate the site labels in central region.
The next step is the computing the RPA interaction within the Dyson and Keldysh equations,

$$V^R(E) = V_0 + V_0\Pi^R(E)V^R(E) \quad (17)$$

$$V^{<,>}(E) = V^R(E)\Pi^{<,>}(E)V^A(E) \quad (18)$$

where $V_0^{<} = 0$. The interacting self-energies are given by the following equations:

$$\Sigma^{<,>}(E) = \tilde{\Sigma}^{<,>}(E) + \tilde{\tilde{\Sigma}}^{<,>}(E) \quad (19)$$

That

$$\tilde{\Sigma}_{kl}^{<,>}(E) = \frac{i}{2\pi}\int dE'\, V_{kl}^{>,<}(E')\, G_{eff,kl}^{<,>}(E-E') \quad (20)$$

and

$$\tilde{\tilde{\Sigma}}_{kk}^{<,>}(E) = -\frac{i}{2\pi}\int dE' \sum_l G_{eff,ll}^{<,>}(E')\, V_{kl}^{>,<}(E) \quad (21)$$

so

$$\sum^{R(\lambda\lambda')}(E) = \frac{i}{2\pi}\int dE' \frac{\sum^{>(\lambda\lambda')}(E') - \sum^{<(\lambda\lambda')}(E')}{E-E'+i0} \quad (22)$$

As shown in Eq. (17), the self-energies $\tilde{\Sigma}^{<,>}$ and $\tilde{\tilde{\Sigma}}^{<,>}$ are the lesser and greater components of the screened potential, $V^{>,<}$, this potential arises from the second-order Coulomb interaction.
We have added the first-order terms to the retarded self-energies in the final results. These first order terms are given by,

$$\tilde{\Sigma}_{kl}^{R(\lambda\lambda')}(E) = \frac{i}{2\pi}\int dE' G_{eff,kl}^{<(\lambda\lambda')}(E-E')\, V_{0,kl}(E') \quad (23)$$

$$\tilde{\tilde{\Sigma}}_{kk}^{R(\lambda\lambda')}(E) = -\frac{i}{2\pi}\int dE' \sum_{l\neq k} G_{eff,ll}^{<(\lambda\lambda')}(E')V_{0,kl} \quad (24)$$

Now, we can obtain the current in interacting systems as follows:

$$J_{int} = \int dE\, Tr[2i\Gamma_L G^R Im(\Sigma_I^{<} G^A f_L) - 2i\Gamma_R G^R Im(\Sigma_I^{<} G^A f_R) + (\Gamma_L - \Gamma_R)G^{<}] \quad (25)$$

Then the spin resolved non-equilibrium and equilibrium charge, can also be determined by the following relations respectively:

$$n_{i\lambda}^{n-eq} = \frac{1}{2\pi}\int dE\left[-iG_{ii}^{<(\lambda\lambda)}(E)\right] \quad (26)$$

$$n_{i\lambda}^{eq} = \frac{-1}{\pi}\int dE\left[Im\, G_{ii}^{R(\lambda\lambda)}(E)\right] \quad (27)$$

where i indicate the site index. Therefore, at a given bias voltage on-site spin polarization can be defined as:

$$\delta n_i(\Delta\mu) = \left(n_{i\uparrow}^{n-eq} + n_{i\uparrow}^{eq}\right) - \left(n_{i\downarrow}^{n-eq} + n_{i\downarrow}^{eq}\right) \quad (28)$$

3. Discussion and results

The influence of the Rashba interaction on the I-V curve of the system has been given in Figure 2 where we have defined $J_0 = \frac{e}{\hbar}t$ and the bias voltage is given by the difference of the chemical potentials of the left and right leads i.e. $\Delta\mu = \mu_L - \mu_R$. Meanwhile $t = 2.66$eV indicates the nearest neighbors hopping parameter in graphene. Negative differential conductance has been defined as a reduction of the system current by increasing the bias voltage. As it can be inferred from Figure 2 (a) and (b) the Rashba interaction can induce negative differential conductance at some specific bias voltages. In addition, as indicated in this figure the Rashba interaction can effectively control the magnitude of the system current. Coulomb interaction introduces several mechanisms in which the conductance of the sample reduces as a result of this interaction. In this way the Coulomb blockade effect, Coulomb induced metal insulator phase transition in half filled magnetic systems could be mentioned. Current study has performed in dilute regime, in which double filling of the local π-states has

been expected to be occur only rarely. In addition, the possibility of double filling could be ignored regarding to the high energy cost for this type charge distribution of the charged particles especially in the dilute regime. Meanwhile since the mobility of the carriers is relatively high in graphene and accordingly the average dwell time of the moving particles, τ_D, in the central system is too short. Therefore, Coulomb blockade of the hopping carriers could not describe the reduction of the conductivity [37].

On the other hand, magnetic configuration of the system, has a dominant contribution in the transport process.

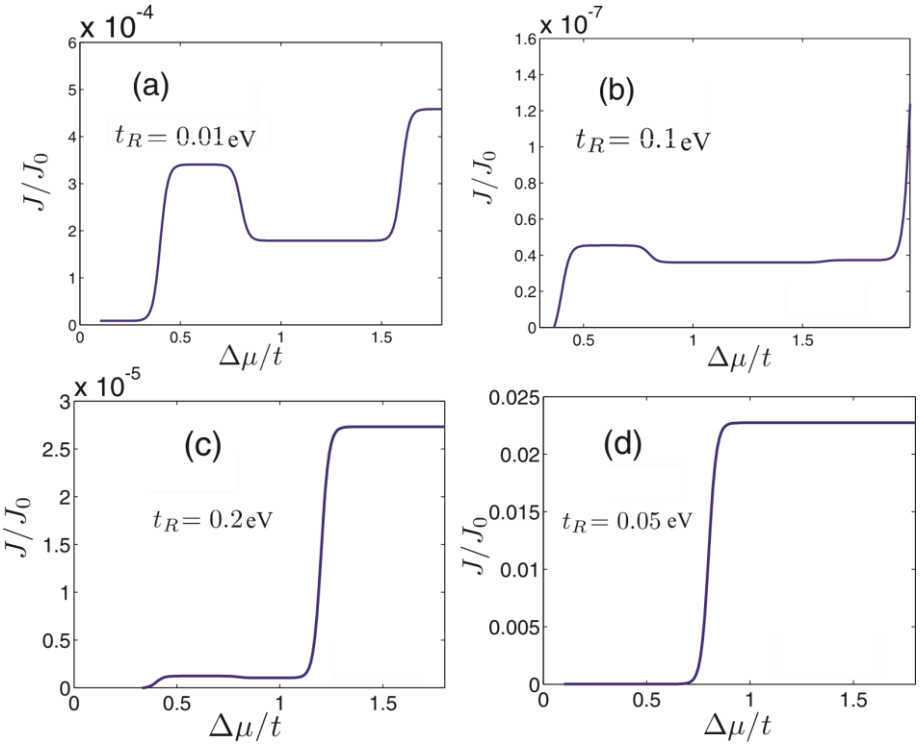

Figure 2. I-V curve of the graphene-based quantum antidot system for different values of Rashba spin-orbit coupling. t_R indicates the strength of the Rashba coupling

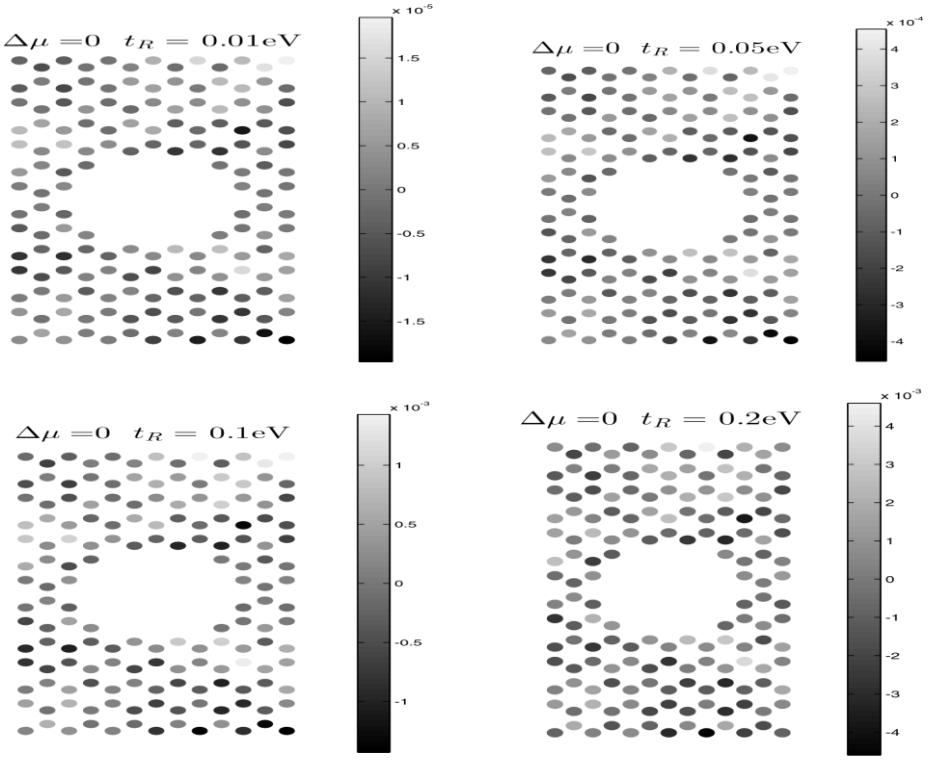

Figure 3. Real space distribution of the spin-accumulation, $n_\uparrow - n_\downarrow$, at different Rashba couplings at zero bias voltage ($\Delta\mu = 0$)

10.57647/jtap.2026.2002.10

The reduction of the conductivity could be described in the presence of the Rashba coupling. If we consider the nonequilibrium spin distribution in the real space one can realize that there is correlation between the electric current and magnetic texture of the system. Meanwhile magnetic configuration of the system could be manipulated by the Rashba interaction. The spin resolved carrier densities have been depicted in Figures 3 and 4. As shown in this figure Rashba coupling and applied bias voltage could effectively modulate the real space distribution of the spin density. At the same time the Rashba interaction modulates the spin flip hopping amplitude.

Within the tight-binding Hamiltonian, if we consider all of the real space possible current carrying paths (which could be considered as all of the paths that could be imagined by nearest-neighbor hoppings) from the left boundary sites to the right boundary.

The transport process could be visualized as a process in which an electron leaves the left boundary and reaches the right boundary by successive hoppings.

A moving carrier has to find a possible path with favorite energy. The on-site spin polarization has been predetermined by the bias voltage at a given Rashba coupling

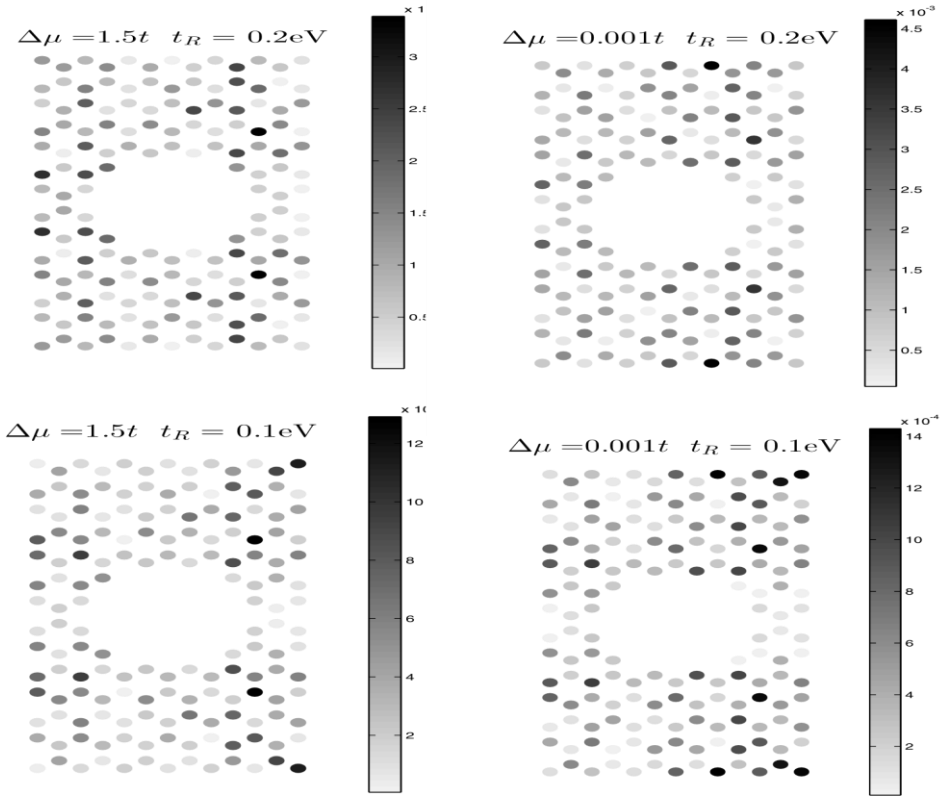

Figure 4. Real space distribution of the spin-accumulation, $|n_\uparrow - n_\downarrow|$, at different bias voltages and Rashba couplings. Darker regions correspond to higher spin densities. This figure indicates that the local spin polarization could be effectively controlled by the Rashba coupling and applied bias voltage

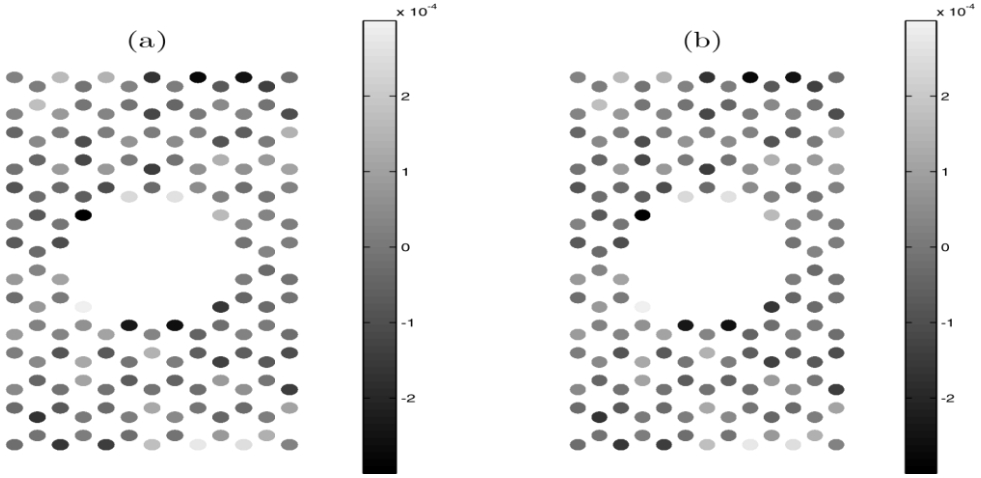

Figure 5. The change of the spin accumulation in a NDC widow at $t_R = 0.1\ eV$. (a) $\delta n_i(0.75t) - \delta n_i(0.6t)$ and (b) $\delta n_i(1.0t) - \delta n_i(0.6t)$

10.57647/jtap.2026.2002.10

Meanwhile the spin of the incoming carrier has also been determined by the Rashba coupling. Since as we mentioned before the spin flip hopping amplitude is determined by the Rashba coupling strength. Therefore, a given current carrying path could be closed when the Rashba coupling leads a moving spin to an atomic site in which there exists an electron with parallel spin. This means that the Rashba coupling can lead some of the current carrying states to a dead end. In the absence of the Rashba coupling, unpolarized spin-current could adjust its magnetic moment with the local magnetization since the hopping process is quite spin-independent. Accordingly, there is not spin-dependent forbidden channels in real-space. By increasing the applied bias voltage, the local spin distribution changes. Accordingly, the number of pathways and the real space distribution of current carrying states could be change by increasing the bias voltage. This can be regarded as main reason of the observed negative differential conductance in the current system. Figure 5 shows the change of the polarization in a NDC bias window. In this figure, In this case $\delta n_i(0.75t)-\delta n_i(0.6t)$ and $\delta n_i(1.0t)-\delta n_i(0.6t)$ measure the change of the spin polarization during and after the NDC region respectively. As indicated in this figure there is a slight correlation between the spin polarization and the electric current. This correlation could be considered a consequence of the spin dependent hopping. We have also obtained the charge accommodation in the current system. Results show that the distribution of the charge accommodation is nearly identical to the distribution of spin accommodation depicted in Figure 3. This is due to the fact that the double filling possibility is very low in this dilutes regime. Since double filling reduces the spin accommodation and increases the charge accommodation in a given real space site and therefore in the low occupation regimes the charge and spin accommodations are nearly identical. As it can be seen in Figure 2 the conductivity of the system has been modulated by the strength of the Rashba interaction. At a given fixed voltage conductivity oscillates by increasing the Rashba coupling. This can be understood if we consider the geometrical Aharonov-Casher phase which could be acquired by moving electron in the presence of the spin orbit Rashba interaction. The Aharonov-Casher could be considered dual effect of the Aharonov-Bohm effect in which the moving magnetic moments acquire path dependent phase in the presence of an electric field where in the current case would be the gate voltage which results in the Rashba type spin orbit coupling. Due to the speed dependent nature of the spin-orbit interactions. It could be expected that the strength of the Rashba interaction which has been felt by an electron should be proportional to the bias voltage which determines the average velocity of the electrons. Accordingly, one might think about the reduction of the electric current as result of the Aharonov-Casher phase shift acquired by a moving magnetic moment. Increasing the bias voltage increases the average longitudinal wave number of the carrier and since the Rashba interaction depends on the velocity of the carriers therefore effective Rashba interaction changes by increasing the bias voltage. It should be noted that the moving electrons could acquire Aharonov-Casher phase shift even at non-adiabatic regimes [38]. This could suggest an alternative mechanism for bias induced current reduction or negative differential conductance. However, results show that this mechanism cannot describe the negative differential conductance since there is no reduction of the electric current when the Coulomb interaction is switched off in the computational modeling. Results of the present work can be employed in design of new type of transistors. Unlike the conventional transistors in which the gate voltage can suppress the conductivity, in this type of transistors the gate voltage which is responsible for the Rashba interaction, can both decrease or increase the conductivity depending on the magnitude of the applied voltage. Therefore, this device could act selectively to the applied bias voltage.

Authors Contribution

All the authors have participated sufficiently in the intellectual content, conception and design of this work or the analysis and interpretation of the data, as well as the writing of the manuscript.

Availability of data and materials

The data that support the findings of this study are available from the corresponding author, upon reasonable request.

Conflict of interests

The authors state that there is no conflict of interest.

References

[1] T.G. Pedersen, C. Flindt, J. Pedersen, N.A. Mortensen, A.P. Jauho, K. Pedersen. “Graphene antidot lattices: Designed defects and spin qubits.” *Physical Review Letters*, 100:136804, 2008. https://doi.org/10.1103/PhysRevLett.100.136804

[2] Y.T. Zhang, Q.M. Li, Y.C. Li, Y.Y. Zhang, F. Zhai. “Band structures and transport properties of zigzag graphene nanoribbons with antidot arrays” *Journal of Physics: Condensed Matter*, 22:315304, 2010. https://doi.org/10.1088/0953-8984/22/31/315304

[3] S.R. Power, A.P. Jauho. “Electronic transport in disordered graphene antidot lattice devices” *Physical Review B*, 90:115408, 2014. https://doi.org/10.1103/PhysRevB.90.115408

[4] A. Manchon, H.C. Koo, J. Nitta, S.M. Frolov, R.A. Duine. “New perspectives for Rashba spin–orbit coupling.”

Nature Materials, 14:871, 2015.
https://doi.org/10.1038/nmat4360

[5] N. Shahabi, A. Phirouznia. "Normal electric field enhanced light-induced polarizations and magnetic detection of valley polarization in silicene" *Scientific Reports*, 10:16612, 2020.
https://doi.org/10.1038/s41598-020-73138-5

[6] K. Hasanirokh, H. Mohammadpour, A. Phirouznia. "Anisotropic quantum transport in monolayer graphene in the presence of Rashba spin–orbit coupling" *Physica E*, 56:227, 2014.
https://doi.org/10.1016/j.physe.2013.09.002

[7] K. Hasanirokh, H. Mohammadpour, M. Esmaelpour, A. Phirouznia. "The Hartman effect in monolayer graphene with Rashba spin–orbit interaction."
https://doi.org/10.1016/j.physe.2015.05.023

[8] F. Rahimi, A. Phirouznia. "Electric field induced pure spin-photo current in zigzag stanene and germanene nanoribbons" *Scientific Reports*, 12:7800, 2022.
https://doi.org/10.1038/s41598-022-11413-3

[9] C. Kane, E. Mele. "Z2 Topological Order and the Quantum Spin Hall Effect." *Physical Review Letters* , 95:146802, 2005.
https://doi.org/10.1103/PhysRevLett.95.146802

[10] Y.A. Bychkov, E.I. Rashba. "Oscillatory effects and the magnetic susceptibility of carriers in inversion layers." *Journal of Physics C: Solid State Physics*, 17:6039, 1984.
https://doi.org/10.1088/0022-3719/17/33/015

[11] S. Ryu, L. Liu, S. Berciaud, Y.J. Yu, H. Liu, P. Kim, G.W. Flynn, L.E. Brus. "Atmospheric oxygen binding and hole doping in deformed graphene on a SiO_2 substrate." *Nano Letters*, 10:4944, 2010.
https://doi.org/10.1021/nl1029607

[12] Y.S. Dedkov, M. Fonin, U. Rüdiger, C. Laubschat. "Rashba Effect in the Graphene/Ni(111) System." *Physical Review Letters* , 100:107602, 2008.
https://doi.org/10.1103/PhysRevLett.100.107602

[13] C. Ertler, S. Konschuh, M. Gmitra, J. Fabian. "Band-structure topologies of graphene: Spin-orbit coupling effects from first principles." *Physical Review B* , 80:235431, 2009.
https://doi.org/10.1103/PhysRevB.80.235431

[14] L. Du, T. Hasan, A. Castellanos-Gomez, G.B. Liu, Y. Yao, C.N. Lau, Z. Sun. "Engineering symmetry breaking in 2D layered materials." *Nature Reviews Physics* , 3:193, 2021.
https://doi.org/10.1038/s42254-020-00276-0

[15] J. Cardoso, P. Pereyra. "Spin inversion devices operating at Fano anti-resonances." *EPL (Europhysics Letters)* , 83:38001, 2008.
https://doi.org/10.1209/0295-5075/83/38001

[16] S. Abdelouahed, A. Ernst, J. Henk, I.V. Maznichenko, I. Mertig. "Spin-split electronic states in graphene: Effects due to lattice deformation, Rashba effect, and adatoms by first principles." *Physical Review B* , 82:125424, 2010.
https://doi.org/10.1103/PhysRevB.82.125424

[17] A. Varykhalov, J.S. Barriga, A.M. Shikin, C. Biswas, E. Vescovo, A. Rybkin, D. Marchenko, O. Rader. "Electronic and Magnetic Properties of Quasifreestanding Graphene on Ni." *Physical Review Letters* , 101:157601, 2008.
https://doi.org/10.1103/PhysRevLett.101.157601

[18] A.H.C. Neto, F. Guinea. "Impurity-induced spin-orbit coupling in graphene." *Physical Review Letters*, 103:026804, 2009.
https://doi.org/10.1103/PhysRevLett.103.026804

[19] Z. Meng, Z. Wu, J. Carrete, Z. Wang. "Twisted bilayer graphene as a linear nanoactuator." *Physical Review B*, 102:155424, 2020.
https://doi.org/10.1103/PhysRevB.102.155424

[20] D.H. Hernando, F. Guinea, A. Brataas. "Spin-orbit coupling in curved graphene, fullerenes, nanotubes, and nanotube caps." *Physical Review B*, 74:155426, 2006.
https://doi.org/10.1103/PhysRevB.74.155426

[21] M. Gmitra, S. Konschuh, C. Ertler, C.A. Draxl, J. Fabian. "Band-structure topologies of graphene: Spin-orbit coupling effects from first principles." *Physical Review B* , 80:235431, 2009.
https://doi.org/10.1103/PhysRevB.80.235431

[22] M. Zarea, N. Sandler. "Rashba spin-orbit interaction in graphene and zigzag nanoribbons." *Physical Review B*, 79:165442, 2009.
https://doi.org/10.1103/PhysRevB.79.165442

[23] M. Inglot, V. Dugaev, E.Y. Sherman, J. Barnaś. "Optical spin injection in graphene with Rashba spin-orbit interaction." *Physical Review B*, 89:155411, 2014.
https://doi.org/10.1103/PhysRevB.89.155411

[24] K. Shakouri, M.R. Masir, A. Jellal, E.B. Choubabi, F.M. Peeters. "Effect of spin-orbit couplings in graphene with and without potential modulation." *Physical Review B*, 88:115408, 2013.
https://doi.org/10.1103/PhysRevB.88.115408

[25] Y.T. Zhang, Q.M. Li, Y.C. Li, Y.Y. Zhang, F. Zhai. "Band structures and transport properties of zigzag graphene nanoribbons with antidot arrays." *J. Phys.: Condens. Matter*, 22(31):315304, 2010.

https://doi.org/10.1088/0953-8984/22/31/315304

[26] A. Manchon, H.C. Koo, J. Nitta, S.M. Frolov, R.A. Duine. "New perspectives for Rashba spin–orbit coupling." *Nat. Mater.*, 14(9):871–882, 2015. https://doi.org/10.1038/nmat4360

[27] R. Kalami, S.A. Ketabi. "Role of linear defects on the electronic, transport, and thermoelectric properties of armchair edge silicene nanoribbons." *J. Electron. Mater.*, 52(7):4644–4654, 2023. https://doi.org/10.1007/s11664-023-10392-z

[28] R. Kalami, S.A. Ketabi. "Electronic and thermoelectric properties of armchair-edge silicene nanoribbons: role of quantum antidot arrays." *J. Electron. Mater.*, 52(10):6566–6577, 2023. https://doi.org/10.1007/s11664-023-10578-5

[29] Berger, Claire, et al. "Electronic confinement and coherence in patterned epitaxial graphene." Science 312.5777 (2006): 1191-1196. https://doi.org/10.1126/science.1125925

[30] Shen, T., et al. "Magnetoconductance oscillations in graphene antidot arrays." *Applied Physics Letters* 93.12 (2008). https://doi.org/10.1063/1.2988725

[31] Kato, Masanori, et al. "Aharonov-Bohm-type oscillations in antidot lattices in the quantum Hall regime." *Physical Review B—Condensed Matter and Materials Physics* 77.15 (2008): 155318. https://doi.org/10.1103/PhysRevB.77.155318

[32] V. Moldoveanu, B. Tanatar. "Spin-dependent transport in graphene-based superlattices." *Physical Review B* , 77:195302, 2008. https://doi.org/10.1103/PhysRevB.77.195302

[33] V. Moldoveanu, B. Tanatar. "Coulomb drag in parallel quantum dots." *EPL (Europhysics Letters)*, 86:67004, 2009. https://doi.org/10.1209/0295-5075/86/67004

[34] H. Haug, A.P. Jauho. "Quantum Kinetics in Transport and Optics of Semiconductors." https://doi.org/10.1007/978-3-540-73564-9

[35] M. Wagner. "Expansions of nonequilibrium Green's functions." *Physical Review B*, 44:6104, 1991. https://doi.org/10.1103/PhysRevB.44.6104

[36] P.L. Sancho, J.L. Sancho, J. Rubio. "Highly convergent schemes for the calculation of bulk and surface Green functions." *Journal of Physics F: Metal Physics*, 15:851, 1985. https://doi.org/10.1088/0305-4608/15/4/009

[37] J. Weis. "Quantum Hall Effect." In *CFN Lectures on Functional Nanostructures Vol. 1*. Springer, pp. 87–121, 2005. https://doi.org/10.1007/978-3-540-31533-9_5

[38] Y. Aharonov, J. Anandan. "Phase change during a cyclic quantum evolution." *Physical Review Letters*, 58:1593, 1987. https://doi.org/10.1103/PhysRevLett.58.1593